nature climate change

Article

https://doi.org/10.1038/s41558-025-02452-5

Multi-century global and regional sea-level rise commitments from cumulative greenhouse gas emissions in the coming decades

Received: 31 October 2024

Accepted: 3 September 2025

Published online: 24 October 2025

Check for updates

Alexander Nauels[1,2] ✉, Zebedee Nicholls[1,2,3], Tessa Möller[1,4], Tim H. J. Hermans[5], Matthias Mengel[6], Uta Kloenne[7], Chris Smith[1,8], Aimée B. A. Slangen[9,10] & Matthew D. Palmer[11,12]

Sea levels respond to climate change on timescales from decades to millennia. To isolate the sea-level contribution of historical and near-term GHG emissions, we use a dedicated scenario and modelling framework to quantify global and regional sea-level rise commitments of twenty-first century cumulative emissions. Under current climate policies, emissions until 2050 lock in 0.3 m (likely range 0.2–0.5 m) more global mean sea-level rise by 2300 than historical emissions until 2020. This additional commitment would grow to 0.8 m (0.5–1.4 m) for emissions until 2090, of which 0.6 m (0.4–1.1 m) could be avoided under very stringent mitigation. Resulting regional commitments would be around 10% higher than the global signal for the vulnerable Pacific region, mainly due to higher relative Antarctic contributions. Our work shows that multi-century sea-level rise commitments are strongly controlled by mitigation decisions in coming decades.

Sea levels respond to GHG emissions and global warming on timescales from decades to millennia. The slow responses of the ocean and ice sheets to elevated surface temperatures lead to substantive global and regional sea-level rise (SLR) commitments for centuries after a cessation of GHG emissions[1]. Apart from the magnitude of long-term SLR, the rate of SLR also determines overall SLR impacts, because coastal risk management and responses have different timescales of planning, implementation and intended lifetime ranging from decades (for example, for ecosystem-based adaptation) to centuries (for example, for planned relocation)[2]. To better inform adaptation planning, the multi-century SLR response must be more comprehensively explored under different emissions futures and at a regional scale[3].

Each additional ton of GHGs emitted in the coming decades locks in more multi-century SLR[4]. This multi-century SLR commitment is directly related to near-term mitigation decisions, including the Nationally Determined Contributions under the UNFCCC[4]. However, most sea-level projections only cover the twenty-first century, due to gaps in process understanding, in particular around ice-sheet instabilities, and high computational costs of running multi-century experiments with complex coupled climate, ocean and ice-sheet models.

Sea-level projections are generally based on scenarios of plausible global emissions trajectories out to 2100. Most of these scenarios come with substantial higher-than-zero emission levels towards the end of this century. These late-century emissions then dominate the

[1]International Institute for Applied Systems Analysis (IIASA), Laxenburg, Austria. [2]Climate & Energy College, School of Geography, Earth and Atmospheric Sciences, The University of Melbourne, Parkville, Victoria, Australia. [3]Climate Resource S, Berlin, Germany. [4]Geography Department, Humboldt-Universität zu Berlin, Berlin, Germany. [5]Institute for Marine and Atmospheric Research Utrecht, Utrecht University, Utrecht, the Netherlands. [6]Potsdam Institute for Climate Impact Research, Potsdam, Germany. [7]Climate Analytics, Berlin, Germany. [8]Department of Water and Climate, Vrije Universiteit Brussel, Brussels, Belgium. [9]Department of Estuarine and Delta Systems, NIOZ Royal Netherlands Institute for Sea Research, Yerseke, the Netherlands. [10]Faculty of Geosciences, Department of Physical Geography, Utrecht University, Utrecht, the Netherlands. [11]Met Office Hadley Centre, Exeter, UK. [12]School of Earth Sciences, University of Bristol, Bristol, UK. ✉e-mail: nauels@iiasa.ac.at

https://doi.org/10.1038/s41558-025-02452-5

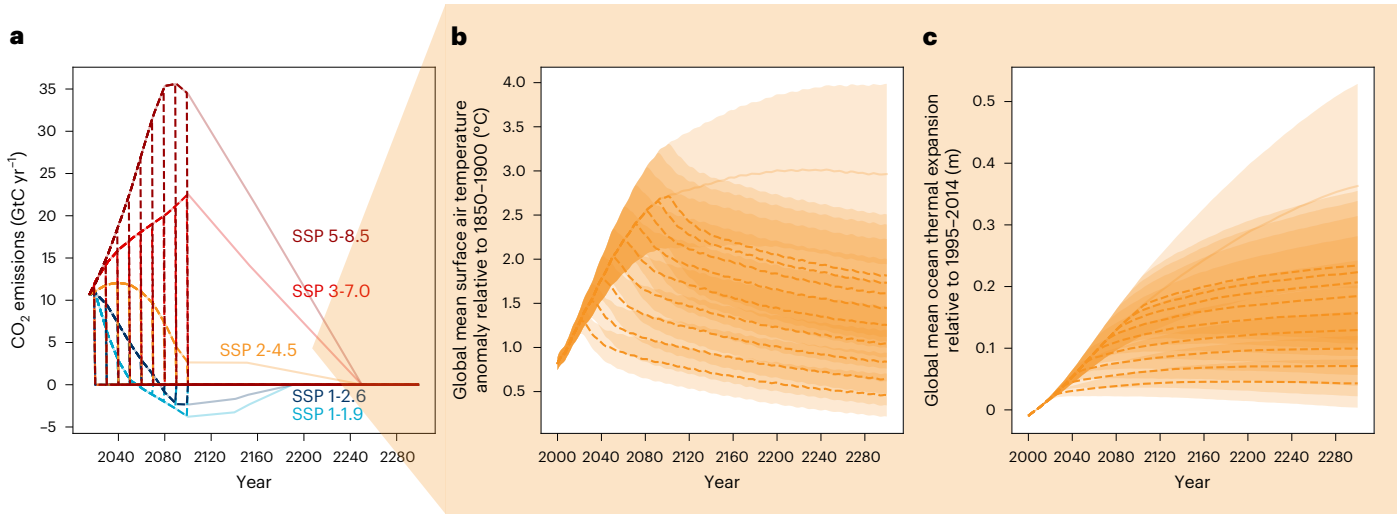

Fig. 1 | Sea-level emulator input data. a, Modified decadal drop-to-zero CO_2 emissions (GtC yr^{-1}) for SSP–RCP commitment scenarios as vertical dashed lines; standard SSP–RCP scenario data shown for comparison as light solid lines. **b**,**c**, Illustrative median global mean surface air temperature anomalies (°C) relative to 1850–1900 (**b**) and illustrative median global mean ocean thermal expansion (in metres sea-level equivalent) relative to 1995–2014 (**c**) under SSP2-4.5-based drop-to-zero commitment scenarios as dashed lines, standard SSP2-4.5 median responses as light solid lines and corresponding 66% model ranges as shaded bands.

longer-term sea-level response and mask the impact of near-term emissions. In this study, we focus on the role of near- and mid-term emissions and investigate their influence on longer-term SLR commitment. This allows us to derive how much SLR will be locked in by near-term emissions alone, highlighting how much committed SLR can be avoided through near-term emissions reductions.

Exploring SLR commitments requires a dedicated scenario setup, in which emissions are zeroed at different times in a large number of emissions pathways. While complex-model experiments exist to investigate zeroing of CO_2 emissions, temperature stabilization and resulting climate system responses[5–7], comparable experiments to systematically investigate sea-level commitments from a zeroing of all GHG emissions are not available. Owing to the large number of scenarios, such a setup would also be difficult to run with computationally expensive Earth system models or complex combined modelling frameworks.

Several sea-level emulators have been developed to project SLR more efficiently[8–13], with individual studies exploring, for example, year-2500 sea-level responses[14] or even 2,000- and 10,000-year SLR commitments[1,15] based on different scenario assumptions. Here we design a set of dedicated SLR commitment scenarios and use them to simulate the global sea-level response with the MAGICC sea-level model[4,9,16]. The global signal is regionalized[12,17] to illustrate regional deviations from the global signal. We explore structural uncertainties of the chosen global method by comparing our results with a complementary, previously published approach (P20)[12]. SLR is projected out to the year 2300 to balance the need to cover as many centuries as possible for capturing a larger fraction of the actual SLR commitment, and the limitations of rapidly increasing uncertainties and knowledge gaps regarding the sea-level response on these longer timescales.

Developing and using SLR commitment scenarios

To investigate SLR commitment, we modify the shared socioeconomic pathway–representative concentration pathway (SSP–RCP) scenario suite assessed in the Intergovernmental Panel on Climate Change (IPCC) Sixth Assessment Report (AR6)[1]. This modified scenario suite forms the basis for exploring the SLR commitment of selected cumulative GHG emission levels under different climate futures throughout the twenty-first century. It includes SSP2-4.5 as a current climate policy-like trajectory and SSP1-1.9 as an emissions reductions pathway consistent with the Paris Agreement. We investigate global and regional changes in year-2300 SLR commitments for emission increases and specific emission levels with a decadal drop-to-zero emissions pathway design (Methods and Fig. 1). The resulting emissions pathways (Fig. 1a) feed into the state-of-the-art simple climate carbon-cycle model MAGICC v.7.5.3 (ref. 18) and the directly coupled MAGICC sea-level model[4,9,16] to generate sea-level projections, and also global mean surface air temperature (GSAT) and global mean ocean thermal expansion (GTE) forcing for the complementary P20 sea-level emulator (Fig. 1b,c). Both MAGICC and P20 include all major SLR drivers (thermal expansion, glaciers, ice sheets and land-water storage) and associated response uncertainties, as captured by the reference data used for the calibration of these emulators.

We use the MAGICC sea-level model[4,9,16] as the main line of evidence for projecting global mean SLR (GMSLR) commitments because it

Table 1 | Projected GMSLR commitments from 2020, 2030, 2050, 2070 and 2090 cumulative GHG emissions based on the SSP–RCP scenarios

Scenario		2300 GMSLR commitments from cumulative GHG emissions until				
		2020	2030	2050	2070	2090
SSP1-1.9	Median	0.29	0.36	0.42	0.44	0.44
	66% range	0.20–0.41	0.24–0.50	0.29–0.60	0.30–0.63	0.30–0.63
	90% range	0.14–0.52	0.19–0.64	0.22–0.80	0.24–0.84	0.24–0.85
SSP1-2.6	Median	0.29	0.37	0.49	0.56	0.58
	66% range	0.20–0.41	0.25–0.51	0.34–0.71	0.39–0.85	0.40–0.89
	90% range	0.14–0.52	0.19–0.65	0.27–0.96	0.30–1.22	0.31–1.29
SSP2-4.5	Median	0.29	0.37	0.58	0.84	1.08
	66% range	0.20–0.41	0.25–0.52	0.41–0.88	0.57–1.38	0.69–1.77
	90% range	0.14–0.52	0.19–0.67	0.31–1.25	0.44–1.95	0.54–2.49
SSP3-7.0	Median	0.29	0.38	0.67	1.20	1.93
	66% range	0.20–0.41	0.26–0.54	0.47–1.06	0.77–1.93	1.24–3.18
	90% range	0.14–0.52	0.20–0.69	0.36–1.54	0.61–2.72	0.96–4.44
SSP5-8.5	Median	0.29	0.39	0.76	1.62	3.02
	66% range	0.20–0.42	0.26–0.55	0.52–1.23	1.01–2.68	1.87–4.98
	90% range	0.14–0.52	0.20–0.71	0.40–1.79	0.78–3.76	1.47–7.16

GMSLR projections are based on the MAGICC sea-level model, displaying medians, 66% (17th to 83 percentile) and 90% (5th to 95th percentile) model ranges in metres relative to 1995–2014.

https://doi.org/10.1038/s41558-025-02452-5

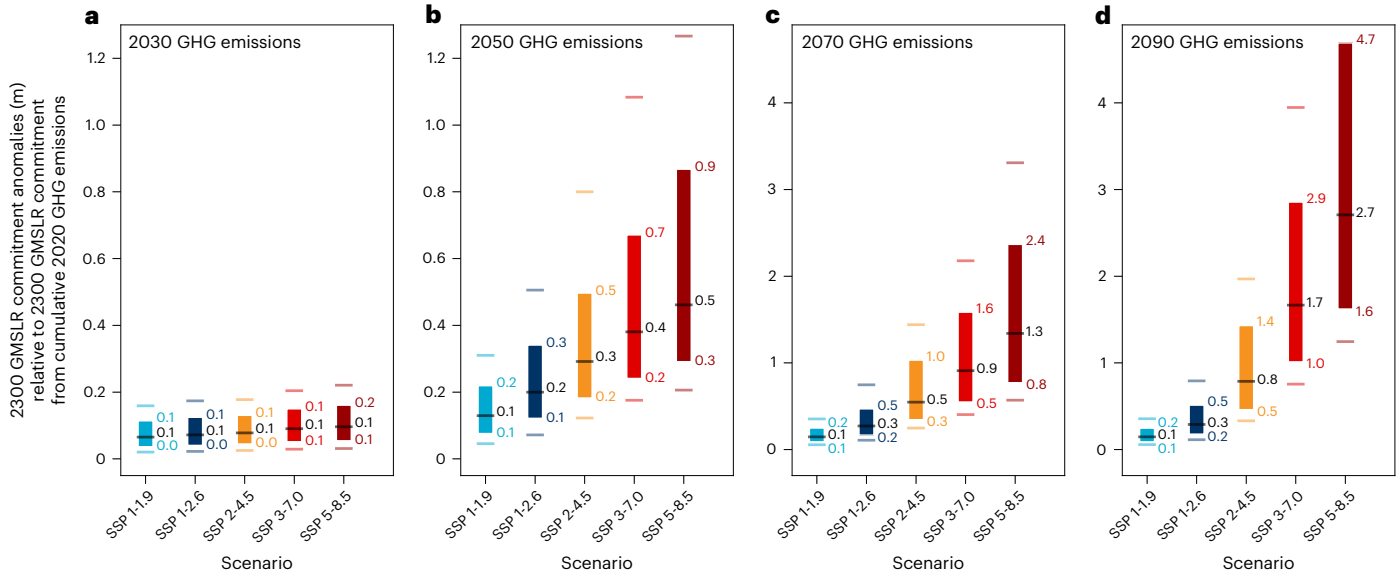

Fig. 2 | 2300 GMSLR commitment anomalies relative to 2300 GMSLR commitment from cumulative GHG emissions until 2020. a–d, 2300 GMSLR commitment anomalies in metres from cumulative 2030 (**a**), 2050 (**b**), 2070 (**c**) and 2090 (**d**) GHG emission levels under the five SSP–RCP-based commitment scenario groups. Boxes capture 66% model ranges, medians are shown by horizontal black lines and coloured whiskers indicate 90% model ranges. For absolute median and model range estimates rounded to two decimals, see Table 1 and Supplementary Fig. 1.

consistently translates GHG emissions to sea-level responses with full scenario flexibility, comes with a more sophisticated model representation of post-2100 GMSLR and uses more recent training data than P20 (ref. 12) (Methods). The MAGICC Greenland and Antarctic components were updated to reflect the IPCC AR6 assessment[1,19–21]. The Antarctic component simulates low-likelihood, high-impact sea-level contributions[13] capturing the AR6 low-confidence projections under high and very high future emissions (Methods and Supplementary Table 4). The approach to derive regional SLR responses[12] accounts for ocean dynamic changes, the Earth's gravitational, rotational and deformational (GRD) response to glacier and ice-sheet melt and present-day glacial isostatic adjustment (GIA) (Methods).

Large structural uncertainties are inherent in the GMSLR commitment projections because they are limited in their ability to fully capture structural differences across reference models and the actual physical mechanisms at play[22], in particular for deeply uncertain ice-sheet processes. Simplified models and their calibrated parametrizations can only reflect the response uncertainties embedded in the reference datasets used for their calibration. The updated MAGICC sea-level emulator is consistent with the IPCC AR6 assessment under the standard SSP–RCP scenarios and its behaviour under the extreme commitment scenarios has been tested (Supplementary Table 1 and Supplementary Section 4). The comparison with the complementary P20 sea-level emulator[12] confirms a plausible sensitivity of the MAGICC GMSLR response to the forcing changes in the commitment scenarios (Discussion, Supplementary Section 2 and Supplementary Table 2).

Global mean SLR commitments

In the following, we show that different shapes of twenty-first century emissions trajectories and corresponding cumulative emission levels translate into a wide range of 2300 GMSLR commitments (Table 1 and Fig. 2). We find that a 2300 GMSLR commitment of 0.20–0.41 m (66% model or likely range, median 0.29 m) relative to 1995–2014 has already been 'locked in' by historical emissions to 2020 (Table 1). These historically committed lower and upper bounds make up 33% and 27% of the lower and upper bounds projected for 2300 by the AR6 under the SSP1-2.6 scenario, respectively, and 9% and 7% under SSP5-8.5. While the additional committed GMSLR in 2300 from emissions between 2020 and 2030 is largely independent of the emissions pathway (Fig. 2a), the effect of the emissions pathway on 2300 GMSLR commitment is clearly emerging midcentury (Fig. 2b–d). By 2050, 0.34 m of the GMSLR commitment in 2300 (median estimate) could be avoided if the world embarked on a 1.5 °C consistent pathway (SSP1-1.9) instead of a very high emissions pathway (SSP5-8.5). Current climate policy-like (SSP2-4.5) emissions until 2050 would commit the world to 0.58 m (0.41–0.88 m) of 2300 GMSLR, which is more than 0.10 m higher than following SSP1-1.9 until the end of the century (2090).

Comparing the 2300 GMSLR commitments from cumulative GHG emissions until 2050, 2070 and 2090 under moderate and higher emissions pathways (SSP2-4.5, SSP3-7.0 and SSP5-8.5), shows that projected GMSLR commitments grow steeply over time. By 2090, a SSP2-4.5 emission trajectory commits the world to 0.64 m (0.39–1.14 m) more GMSLR in 2300 compared with the most stringent mitigation pathway SSP1-1.9 (Table 1 and Fig. 2). For the highest cumulative GHG emissions until 2090 (SSP5-8.5), the 2300 GMSLR commitment reaches up to around 7 m for the upper bounds of the very likely (90%) range (Table 1), highlighting the escalation of GMSLR associated with continued very high GHG emissions under a low-likelihood, high-impact storyline. Under SSP1-1.9, however, the 2300 GMSLR commitment from 2090 GHG emissions could be limited to 0.44 m (0.30–0.63 m), underscoring the opportunity to avoid substantial long-term GMSLR commitment through ambitious mitigation measures.

Relating SLR commitments to carbon budgets and peak warming

We relate 2300 GMSLR commitments to cumulative net-positive CO_2 emissions, that is cumulative emissions until a CO_2 emissions pathway reaches net-zero, and to the 1.5 °C (50% likelihood) and 2 °C (67% likelihood) carbon budgets (Fig. 3a). The results further highlight the multi-century legacy of emissions reductions decisions taken today. The difference in best-estimate cumulative CO_2 emissions between the 1.5 °C (50% likelihood, in green) and 2 °C (67% likelihood, in blue) carbon budgets translates into a 2300 GMSLR commitment difference of more than 0.5 m, when looking at the highest ensemble members.

https://doi.org/10.1038/s41558-025-02452-5

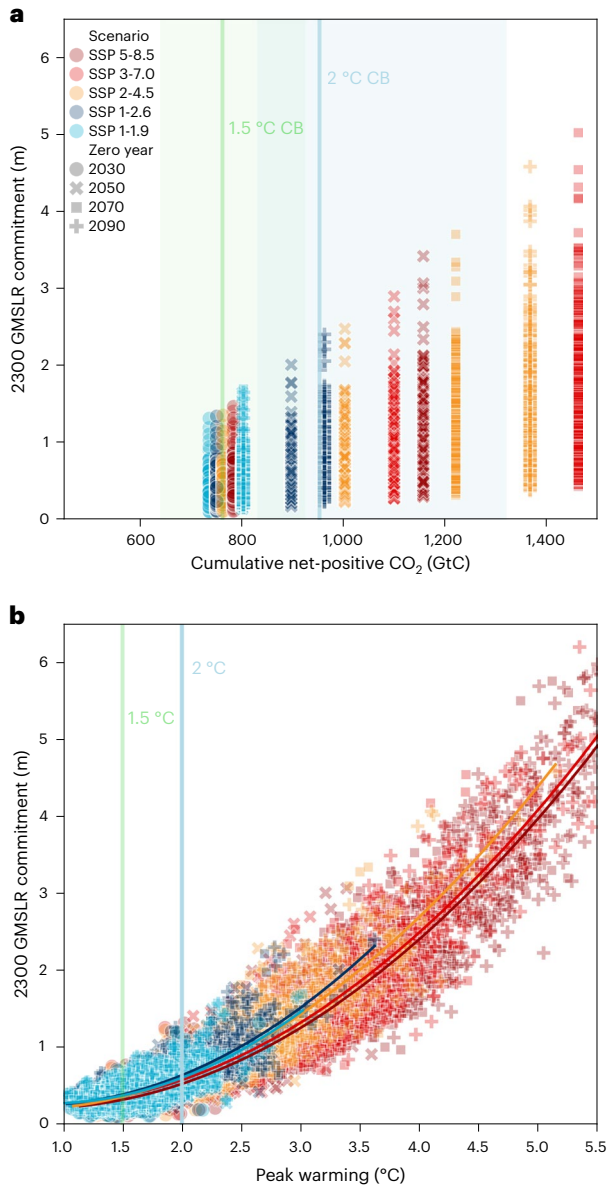

Fig. 3 | 2300 GMSLR commitments related to cumulative net-positive CO_2 emissions and peak warming. a,**b**, Individual 2300 GMSLR commitment ensemble members in metres relative to 1995–2014 coloured by SSP–RCP-based commitment scenario groups (symbols indicate different zero years) related to: cumulative net-positive CO_2 emissions and carbon budgets (CB) for 1.5 °C (50% likelihood as vertical light green line) and 2 °C (67% likelihood as vertical light blue line), with CB likely ranges including observational uncertainty as shaded bands[2,36] (**a**); and to peak warming (°C) relative to 1850–1900, with quadratic fits shown for each SSP–RCP commitment scenario group (**b**).

We also examine 2300 GMSLR commitments and peak warming (Fig. 3b). A nonlinear relationship between GMSLR and temperature change emerges, as illustrated by the quadratic fits per SSP–RCP commitment scenario group, consistent with other findings comparing GMSLR and time-integrated temperature change[23]. The increasing sensitivity with warming can be attributed to a nonlinear increase in ice mass loss in a warmer world. This feature is only visible on a multi-century time horizon, when ice sheets have time to respond to atmospheric warming. The wide spread of the GMSLR commitments in Fig. 3b underscores the large uncertainty in multi-century SLR projections, with the upper end of the full GMSLR commitment ranges increasingly exceeding 2 m for peak warming outcomes beyond around 2.5 °C (Fig. 3b).

Regional SLR commitment

Regional SLR commitments are relevant for the assessment of coastal hazards, adaptation needs and loss and damage, especially for vulnerable regions such as Small Island Developing States. Therefore, we show regional SLR responses (Methods) for two scenarios (SSP1-1.9 and SSP2-4.5), two maps for the regional SLR patterns resulting from 2050 GHG emissions and time series for four illustrative tide gauge stations based on the applied regionalization method[12] (Fig. 4).

There is a strong regional signal in committed SLR due to processes such as ocean dynamics, GRD effects of glaciers and ice-sheet mass loss and GIA (Fig. 4a,g). Our results, in some cases even showing a negative sea-level response, underscore that a detailed assessment of the GRD effects and GIA of the Earth, as well as other processes contributing to vertical land motion (VLM) that we did not consider here, is crucial to determine the regional climate-driven SLR commitment in combination with non-climate-driven changes.

As an example, New York (USA) will experience substantially higher than global SLR commitments under both SSP1-1.9 and SSP2-4.5 trajectories (Fig. 4d,j). Of the four selected illustrative tide gauge stations, New York is the only location that shows positive contributions from GIA under both scenarios. Under SSP2-4.5, a larger than global Antarctic contribution further amplifies the above-GMSLR effect, while Greenland only plays a negligible role due to the geographical proximity to this ice sheet.

Under the current climate policy-like (SSP2-4.5) commitment scenario, Pago Pago (American Samoa) also shows higher than global 2300 SLR commitment estimates (Fig. 4l). This signal is mainly driven by larger relative contributions from the Antarctic ice sheet and would be in line with overall findings that Pacific small island nations will experience SLR that is around 10% higher than the global mean[24].

The results for Oslo (Norway) demonstrate the regional effects of land uplift driven by GIA (Fig. 4e,k). These effects dominate regional sea-level changes for Scandinavian locations as well as high-latitude North American locations. Oslo shows a negative SLR under all SSP1-1.9 projections. Similarly, the SSP2-4.5 commitment scenarios result in a sea level fall by 2300, while the standard SSP2-4.5 pathway leads to positive 2300 SLR. Here, the local vertical land uplift exceeds the climate-driven SLR commitment signal in the drop-to-zero cases.

Both scenario setups show that large areas in the Pacific, South Atlantic and Indian Ocean experience higher-than-global regional SLR commitment (Fig. 4a,g) due to above-average regional contributions from ice-sheet mass loss, particularly from Antarctica, glacier mass loss, sterodynamic changes or a combination of those drivers[16]. For all locations, differences between the time series of committed 2300 SLR from 2090, 2050 and 2030 emissions (dashed lines) are much smaller under the most ambitious climate mitigation scenario (SSP1-1.9) and do not deviate much from the SLR projections for the standard scenario (solid lines). The small differences in the SSP1-1.9 projections are due to a much larger SLR fraction that is not sensitive to the cessation of emissions throughout the twenty-first century, but driven by already committed contributions from thermal expansion, glaciers and ice sheets. These add to GRD and GIA contributions that are less sensitive to changes in climate.

Discussion

The applied SLR commitment approach isolates the SLR signal of historical, near- and mid-term GHG emissions and differs from studies that are based on non-zero emissions trajectories beyond the cumulative emission levels of interest[25]. The setup assumes that the sea-level models handle the sudden GHG emissions drop in a physically plausible way. For the slow sea-level response, the climate forcing strongly cushions the step-change signal from the commitment scenarios. The sea-level emulator adopts the behaviour of the calibrated GMSLR response under strong emissions reductions and lowers the commitment projections roughly equivalent to the difference between

https://doi.org/10.1038/s41558-025-02452-5

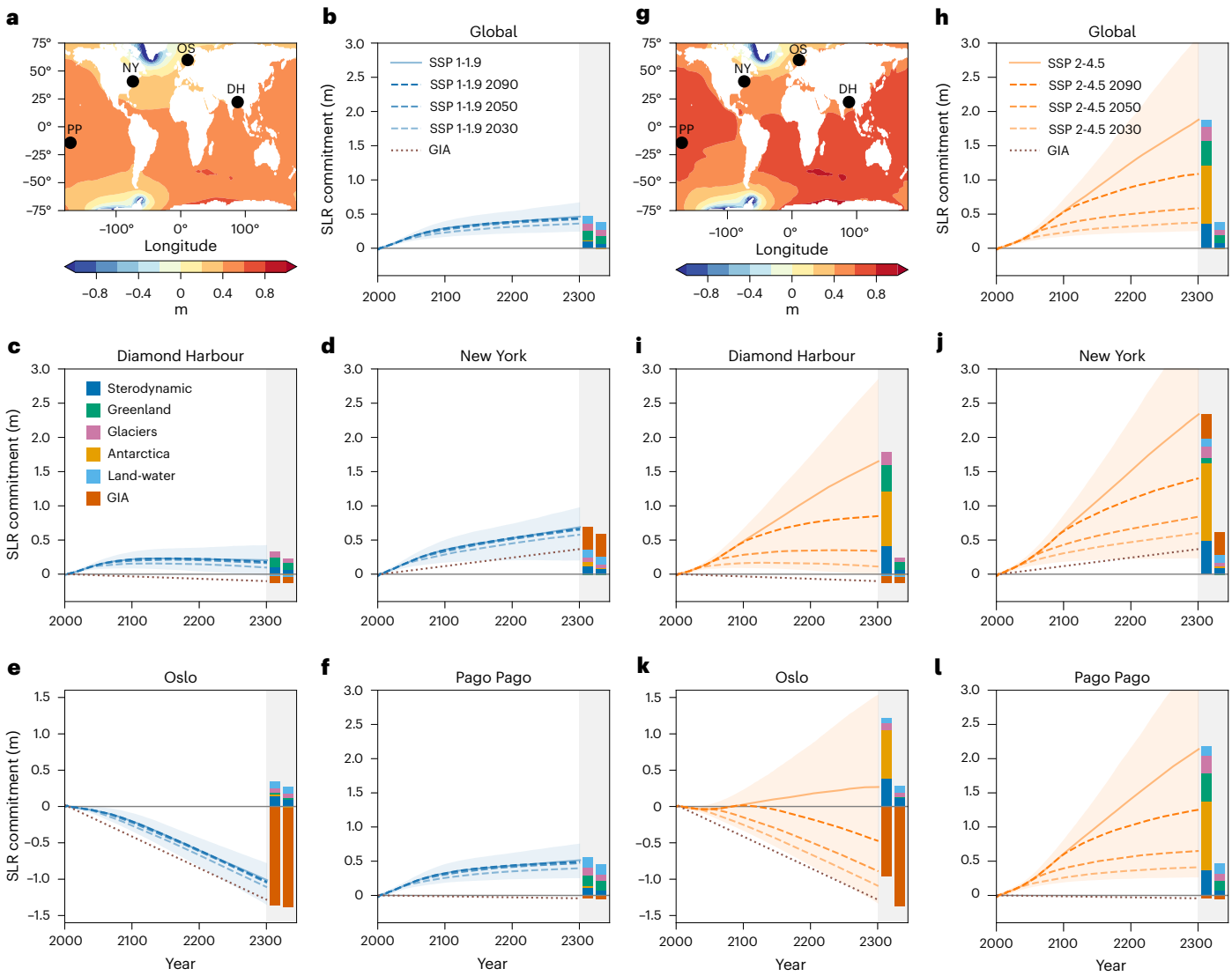

Fig. 4 | Regional SLR commitments. Maps of 2300 regional SLR commitments resulting from cumulative 2050 GHG emissions under SSP1-1.9 (**a**) and SSP2-4.5 (**g**) in metres relative to 1995–2014, excluding glacial isostatic adjustment. MAGICC GMSLR time series with overall 66% model ranges for SSP1-1.9 (**b**) and SSP2-4.5 (**h**) commitment scenario groups, medians for the standard scenario (solid line) and commitment variants with zeroed emissions in 2090, 2050 and 2030 (dashed lines). Local SLR commitment time series with overall 66% model range and medians for the respective scenario groups at the illustrative regional sites Diamond Harbour (DH) (**c**,**i**), New York (NY) (**d**,**j**), Oslo (OS) (**e**,**k**) and Pago Pago (PP) (**f**,**l**). Vertical bars show the median 2300 SLR contributions per component for the baseline SSP–RCP scenario (left bars) and the 2030 SLR commitment variant (right bars): sterodynamic/thermal expansion, blue; Greenland, green; glaciers, magenta; Antarctica, orange; land-water, light blue; and GIA, vermilion.

cumulative emissions levels from commitment and the corresponding calibration scenario. The ability to robustly estimate GMSLR commitments is further tested by applying an out-of-sample experiment to the Greenland sea-level component, which is highly sensitive to scenario choice (Supplementary Section 4), increasing confidence in the presented sea-level responses to such extreme changes in emissions. While we expect the other model components to behave similarly to the Greenland component, a more systematic analysis of sea-level emulators and their behaviour under out-of-sample scenarios should be carried out in the future, with a particular focus on ice-sheet responses.

We use simple models calibrated against complex models, for both the climate and sea-level responses, to enable the analysis of our commitment scenario set. MAGICC v.7.5.3 was calibrated to coupled model intercomparison project phase 6 (CMIP6) climate data and widely used in the IPCC AR6 report[18,26,27]. The MAGICC sea-level model has been applied and evaluated out to the year 2300 under many different scenarios[4,9,16]. The updated MAGICC sea-level model shows overall consistency with the IPCC AR6 GMSLR assessment for the standard SSP–RCP scenario set, resulting in lower projections under lower emissions scenarios than the previous model version (Supplementary Tables 1 and 3–8). MAGICC captures the lower end of the IPCC AR6 assessed GMSLR range under low and very low emissions pathways (SSP1-2.6 and SSP1-1.9), which also results in lower 2300 GMSLR commitment projections than the complementary P20 approach under SSP1-2.6. The latter can only be run with a subset of the commitment scenarios and shows a lower sensitivity to reductions in climate forcing. For higher emissions scenarios, MAGICC emulates a much stronger acceleration in the Antarctic GMSLR contribution than the P20 approach, reflecting the plausible but highly uncertain risk of very large Antarctic ice mass loss. The corresponding MAGICC likely range for the 2300 Antarctic sea-level response under very high emissions (SSP5-8.5: 4.70–10.05 m) captures the state-of-the-art Ice Sheet Model Intercomparison Project maximum

estimate, including ice-shelf collapse, of 6.9 m sea-level equivalent[28]. By deliberately simulating an Antarctic sea-level response in line with the low-likelihood, high-impact IPCC AR6 assessment[1,20], we highlight the rapidly increasing SLR risk from unmitigated GHG emissions. The MAGICC sea-level model is able to reflect complex physical dynamics through, for example, threshold temperature parametrizations[16], but it cannot fully resolve physical processes such as the nonlinear response of West Antarctic glaciers to local warming[1,29]. For the main GMSLR commitment results presented in Fig. 2, we show anomalies relative to the reference GMSLR commitment from 2020 emissions. These anomalies can be attributed more easily to differences in future climate forcing. Absolute values are subject to the additional uncertainties underlying present-day estimates.

We use fingerprints for the regionalization of the sea-level response, assuming a static relation between the global and local signals[12], drawing from previous regionalization efforts[17]. There are substantial uncertainties associated with the translation of globally aggregated ocean heat content and thermal expansion to local ocean dynamic sea-level change, in particular when extrapolating to 2300 (refs. 1,30,31). Our estimates are derived from large-scale climate models, so they have limited predictive capacity for specific coastal locations. For these, coastal dynamics and also discharge around river estuaries play important roles that cannot be assessed here as they require high-resolution simulations and dynamical downscaling[32,33]. In addition, VLM is a major factor in local sea-level change, but it is highly varying, both spatially and temporally, and driven by a wide range of processes (for example, GIA, subsidence, tectonics and anthropogenic drivers such as groundwater withdrawal). An assessment of regional VLM other than caused by GIA[12] is also beyond the scope of this study.

There is tension between the need to explore long-term changes and the limited understanding of sea-level processes on these timescales. This is particularly true for sea-level rise after 2100 on regional to local spatial scales. We acknowledge this but argue that it should not prevent the exploration of multi-century SLR commitments, since only the commitment perspective brings to the fore the large influence of the emissions of today on the sea-level system, which is of high societal relevance. The severe SLR threat for small islands and vulnerable coastal areas, and the need to support much-needed assessments of adaptation requirements and loss and damage[34,35], requires multi-century SLR assessments to capture a larger fraction of the sea-level response.

More complex, process-based, multi-centennial sea-level simulations, also under maximum mitigation and overshoot scenarios, would help to narrow down the uncertainties in studies such as ours. Future research should compare and test available sea-level emulators more systematically, in particular on multi-century timescales, to advance scientific methods and understanding of uncertainty. Ultimately, more sea-level emulator studies are needed to grow the sea-level attribution literature and facilitate economic and non-economic damage assessments.

Within the stated limitations, our approach provides an opportunity to explore the SLR committed by cumulative emissions in the near future, on timescales that, compared with the common twenty-first century focus, capture a larger fraction of the true SLR response. This study establishes a more direct link between climate change mitigation decisions taken in the coming decades and the resulting multi-century SLR response to ultimately better inform mitigation and adaptation planning. Our results reinforce how every increment of additional peak warming from cumulative emissions irreversibly increases SLR. This emphasizes the importance of aligning global emissions with a Paris Agreement consistent pathway, and underscores that stringent GHG mitigation needs to start today.

Online content

Any methods, additional references, Nature Portfolio reporting summaries, source data, extended data, supplementary information, acknowledgements, peer review information; details of author contributions and competing interests; and statements of data and code availability are available at https://doi.org/10.1038/s41558-025-02452-5.

References

1. Fox-Kemper, B. et al. in *Climate Change 2021: The Physical Science Basis* (eds Masson-Delmotte, V. et al.) 1211–1362 (Cambridge Univ. Press, 2021).
2. *Climate Change 2023: Synthesis Report* (eds Core Writing Team, Lee, H. & Romero, J.) 35–115 (IPCC, 2023).
3. Haasnoot, M. et al. Long-term sea-level rise necessitates a commitment to adaptation: a first order assessment. *Clim. Risk Manag.* **34**, 100355 (2021).
4. Nauels, A. et al. Attributing long-term sea-level rise to Paris Agreement emission pledges. *Proc. Natl Acad. Sci. USA* **116**, 23487–23492 (2019).
5. Jones, C. D. et al. The Zero Emissions Commitment Model Intercomparison Project (ZECMIP) contribution to C4MIP: quantifying committed climate changes following zero carbon emissions. *Geosci. Model Dev.* **12**, 4375–4385 (2019).
6. Sigmond, M., Fyfe, J. C., Saenko, O. A. & Swart, N. C. Ongoing AMOC and related sea-level and temperature changes after achieving the Paris targets. *Nat. Clim. Change* **10**, 672–677 (2020).
7. King, A. D. et al. Exploring climate stabilisation at different global warming levels in ACCESS-ESM-1.5. *Earth Syst. Dynam.* **15**, 1353–1383 (2024).
8. Mengel, M. et al. Future sea level rise constrained by observations and long-term commitment. *Proc. Natl Acad. Sci. USA* **113**, 201500515 (2016).
9. Nauels, A., Meinshausen, M., Mengel, M., Lorbacher, K. & Wigley, T. M. L. Synthesizing long-term sea level rise projections—the MAGICC sea level model v2.0. *Geosci. Model Dev.* **10**, 2495–2524 (2017).
10. Wong, T. E. et al. BRICK v0.1, a simple, accessible, and transparent model framework for climate and regional sea-level projections. *Geosci. Model Dev. Discuss.* **2017**, 1–36 (2017).
11. Kopp, R. E. et al. Evolving understanding of Antarctic ice-sheet physics and ambiguity in probabilistic sea-level projections. *Earth's Future* **5**, 1217–1233 (2017).
12. Palmer, M. D. et al. Exploring the drivers of global and local sea-level change over the 21st century and beyond. *Earth's Future* **8**, e2019EF001413 (2020).
13. van de Wal, R. S. W. et al. A high-end estimate of sea level rise for practitioners. *Earth's Future* **10**, e2022EF002751 (2022).
14. Turner, F. E. et al. Illustrative multi-centennial projections of global mean sea-level rise and their application. *Earth's Future* **11**, e2023EF003550 (2023).
15. Clark, P. U. et al. Consequences of twenty-first-century policy for multi-millennial climate and sea-level change. *Nat. Clim. Change* **6**, 360–369 (2016).
16. Nauels, A., Rogelj, J., Schleussner, C.-F., Meinshausen, M. & Mengel, M. Linking sea level rise and socioeconomic indicators under the Shared Socioeconomic Pathways. *Environ. Res. Lett.* **12**, 114002 (2017).
17. Slangen, A. B. A. et al. Projecting twenty-first century regional sea-level changes. *Clim. Change* **124**, 317–332 (2014).
18. Forster, P. et al. in *Climate Change 2021: The Physical Science Basis* (eds Masson-Delmotte, V. et al.) 923–1054 (Cambridge Univ. Press, 2021).
19. Greve, R. & Chambers, C. Mass loss of the Greenland ice sheet until the year 3000 under a sustained late-21st-century climate. *J. Glaciol.* **68**, 618–624 (2022).
20. Edwards, T. L. et al. Revisiting Antarctic ice loss due to marine ice-cliff instability. *Nature* **566**, 58–64 (2019).

21. Golledge, N. R. et al. Global environmental consequences of twenty-first-century ice-sheet melt. *Nature* **566**, 65–72 (2019).
22. Lehner, F. et al. Partitioning climate projection uncertainty with multiple large ensembles and CMIP5/6. *Earth Syst. Dynam.* **11**, 491–508 (2020).
23. Hermans, T. H. J. et al. Projecting global mean sea-level change using CMIP6 models. *Geophys. Res. Lett.* **48**, e2020GL092064 (2021).
24. Sadai, S., Spector, R. A., DeConto, R. & Gomez, N. The Paris Agreement and Climate Justice: inequitable impacts of sea level rise associated with temperature targets. *Earth's Future* **10**, e2022EF002940 (2022).
25. Mengel, M., Nauels, A., Rogelj, J. & Schleussner, C.-F. Committed sea-level rise under the Paris Agreement and the legacy of delayed mitigation action. *Nat. Commun.* **9**, 601 (2018).
26. Lee, J.-Y. et al. in *Climate Change 2021: The Physical Science Basis* (eds Masson-Delmotte, V. et al.) 553–672 (Cambridge Univ. Press, 2021).
27. Chen, D. et al. in *Climate Change 2021: The Physical Science Basis* (eds Masson-Delmotte, V. et al.) 147–286 (Cambridge Univ. Press, 2021).
28. Seroussi, H. et al. Evolution of the Antarctic ice sheet over the next three centuries from an ISMIP6 model ensemble. *Earth's Future* **12**, e2024EF004561 (2024).
29. Van Den Akker, T. et al. Present-day mass loss rates are a precursor for West Antarctic ice sheet collapse. *Cryosphere* **19**, 283–301 (2025).
30. Malagón-Santos, V. et al. Improving statistical projections of ocean dynamic sea-level change using pattern recognition techniques. *Ocean Sci.* **19**, 499–515 (2023).
31. Yuan, J. & Kopp, R. E. Emulating ocean dynamic sea level by two-layer pattern scaling. *J. Adv. Model. Earth Syst.* **13**, e2020MS002323 (2021).
32. Hermans, T. H. J. et al. Drivers of interannual sea level variability on the Northwestern European Shelf. *J. Geophys. Res. Oceans* **125**, e2020JC016325 (2020).
33. Chaigneau, A. A. et al. Impact of sea level changes on future wave conditions along the coasts of western Europe. *Ocean Sci.* **19**, 1123–1143 (2023).
34. Martyr-Koller, R., Thomas, A., Schleussner, C.-F., Nauels, A. & Lissner, T. Loss and damage implications of sea-level rise on small island developing states. *Curr. Opin. Environ. Sustain.* **50**, 245–259 (2021).
35. Martyr-Koller, R. & Schleussner, C.-F. Coastal loss and damage for small islands. *Nat. Sustain.* **6**, 1508–1509 (2023).
36. Forster, P. M. et al. Indicators of Global Climate Change 2023: annual update of key indicators of the state of the climate system and human influence. *Earth Syst. Sci. Data* **16**, 2625–2658 (2024).

Methods

Commitment scenarios

The five SSP–RCP scenarios (SSP1-1.9, SSP1-2.6, SSP2-4.5, SSP3-7.0 and SSP5-8.5)[37] are used as the basis for the SLR commitment scenario framework to capture the full breadth of emissions trajectories assessed in IPCC AR6 Working Group I (ref. 28). Until 2014, the applied climate model derives GHG emissions on the basis of the CMIP6 historical GHG concentrations. Starting in 2015, the SSP–RCP emissions of 43 GHGs are used as forcing input. At the start of every decade between 2020 and 2100, all Kyoto GHGs (CO_2, CH_4, N_2O and fluorinated gases) are set to zero, while emissions from other substances (SO_2, NO_x, CO, organic carbon, non-methane volatile organic compounds, black carbon and NH_3) are gradually phased out. Building on previous work[4], an exponential 45-year phase-out is used to prevent a sudden temperature spike after the year of zeroing Kyoto GHGs due to the abrupt removal of substances with short-term climate effects. Applying the decadal drop-to-zero emissions approach to all five SSP–RCPs and running the unmodified baseline SSP–RCPs for comparison, results in a total of 50 emissions pathways analysed in this study.

MAGICC global climate and sea-level model

The simple climate carbon-cycle model MAGICC v.7.5.3 (ref. 37) is used in its IPCC AR6 setup[18] to translate the GHG emissions trajectories from the commitment scenarios into GSAT and GTE projections. The MAGICC sea-level model[4,9,16] is run as part of MAGICC v.7.5.3 and provides GMSLR estimates from 1850 to 2300. While the model can be run beyond 2300, the time frame is not extended further because of a lack of process-based reference datasets. The MAGICC sea-level model emulates process-based SLR projections for all major climate-driven components: thermal expansion, global glacier mass changes, surface mass balance and solid-ice discharge from the Greenland and Antarctic ice sheets, as well as the non-climate-driven contribution from land-water storage. For each of the 600 probabilistic ensemble members derived by a Metropolis–Hastings Markov chain Monte Carlo method[38], calibrated sea-level parameters are randomly selected for the individual sea-level component parametrizations. The solid-ice discharge component of the Antarctic ice sheet has been recalibrated to capture revised projections that simulate very rapid Antarctic ice mass loss[20] to capture a low-likelihood, high-impact storyline consistent with the IPCC AR6 low-confidence SLR assessment under high emissions scenarios. The Antarctic surface mass balance as well as the Greenland surface mass balance and solid-ice discharge components of the MAGICC sea-level model have also been updated and recalibrated with more recent reference data[19,21]. For the Greenland surface mass balance component, a threshold temperature was implemented in the parametrization to capture the GSAT increase for which the surface mass balance would switch from a negative to a positive GMSLR contributor based on published estimates[39]. In addition, the land-water storage component has been revised to reproduce the IPCC AR6 assessment[1].

Regional sea-level model

The applied regionalization[12] draws from the projected GMSLR contributions from the individual MAGICC sea-level components (thermal expansion, glaciers, Greenland and Antarctic ice sheets and land-water storage) and considers additional relevant processes. First, the spatial patterns of mean sea-level (MSL) change related to each barystatic GMSL contribution are integrated, incorporating estimates of GRD effects. Following previous studies[17,40–42], local changes in ocean density and circulation are derived via linear regression relationships between GTE and local sterodynamic sea-level change in CMIP5 climate model simulations. Supplementary Table 7 compares globally aggregated thermal expansion estimates by updated MAGICC/P20 approaches with the IPCC AR6 Working Group I. Aggregated CMIP5 and CMIP6 thermal expansion information is largely consistent, with CMIP6 showing a slightly larger spread while median information is very similar[23]. We therefore consider older CMIP5 thermal expansion information to be sufficient to explore the regional signal, given the simplifications assumed as part of the chosen approach. Finally, the spatial pattern of local MSL change resulting from ongoing GIA is incorporated into the regional SLR projections. Projections of local MSL change for specific tide gauge locations are directly derived from the global sea-level projections. The local MSL projection Monte Carlo simulations are computed from a single randomly selected instance of the 450,000-member Monte Carlo ensemble of GMSL. Each instance contains a time series for the seven GMSL components that retains the underlying correlations between them. The barystatic time series are paired with the corresponding GRD estimates at the latitude and longitude of the tide gauge. These pairings are randomly drawn, with all GRD patterns based on the same model to preserve correlated errors. The only exception is land-water, for which only one GRD estimate is available[17]. The time series of global thermal expansion is combined with a randomly drawn regression coefficient from one of the 21 CMIP5 models to estimate the sterodynamic sea-level change at the tide gauge location. The resulting time series of local MSL change are then combined with an estimate of the rate of MSL change associated with GIA using one of the estimates drawn at random. This procedure is repeated 100,000 times for each tide gauge location to build up a distribution of MSL projections under each scenario. Four illustrative tide gauge locations are selected to capture a broad range of regional sea-level responses and to showcase regional SLR commitments: New York City (USA), Oslo (Norway), Diamond Harbour (India) and Pago Pago (American Samoa). The spatial maps shown in Fig. 4 are built on methods used for Fig. 13.16 in ref. 43 and Fig. 2 in ref. 12.

Complementary P20 global sea-level model

The GMSLR projections by ref. 12 (P20) are composed of the seven components global mean thermal expansion, Antarctic surface mass balance, Antarctic ice dynamics, Greenland surface mass balance, Greenland ice dynamics, global glaciers and changes in land-water storage. The components reproduce the IPCC AR5 GMSLR assessment, except for the Antarctic ice dynamics, which have been updated to emulate scenario-dependent responses[44]. More recent work has highlighted the potential importance of self-sustaining dynamic ice feedbacks[45,46], which are not explicitly accounted for by the update. However, the P20 update yields a similar projected range to other recent studies that can reproduce these effects[20]. The 2100 GMSLR projections are drawing from the GTE and GSAT changes produced by the CMIP6-consistent MAGICC v.7.5.3 under the SLR commitment scenarios designed for this study. Only SSP1-2.6, SSP2-4.5 and SSP5-8.5 commitment scenario forcing is fed into the P20 approach because its Antarctic ice dynamic component draws from RCP2.6, RCP4.5 and RCP8.5 scenarios, which are roughly equivalent to the corresponding SSP–RCPs in terms of climate forcing. The extended 2300 projections use GTE and GSAT change projections from a physical emulator that has been calibrated to 16 CMIP5 models[42] under the RCP extensions[47]. The different GMSL components are combined using a 450,000-member Monte Carlo simulation that samples from the underlying distributions. The procedure preserves the correlation between GTE and GSAT change in the underlying model ensembles. More details on the methods used for each component and for the two different time horizons can be found in the original study[12]. The P20 GMSLR outputs are compared with MAGICC GMSLR projections and the IPCC AR6 Working Group I GMSLR assessment[1] in Supplementary Section 2 and Supplementary Tables 1 and 3–6.

Data availability

The data underlying the study are available via Zenodo at https://doi.org/10.5281/zenodo.16572777 (ref. 48). Supporting code to explore and reproduce the results and figures presented in this study can be accessed via https://gitlab.com/anauels/slr_commitment.

Code availability

The MAGICC source code is available at https://gitlab.com/magicc/magicc. The code underlying the regionalization can be found at https://github.com/MetOffice/ProFSea-tool. The code underlying the complementary P20 global sea-level approach can be accessed via https://github.com/JonathanGregory/ar5gmslr.

References

37. Meinshausen, M. et al. The shared socio-economic pathway (SSP) greenhouse gas concentrations and their extensions to 2500. *Geosci. Model Dev.* **13**, 3571–3605 (2020).
38. Meinshausen, M. et al. Greenhouse-gas emission targets for limiting global warming to 2 °C. *Nature* **458**, 1158–1162 (2009).
39. Noël, B., Van Kampenhout, L., Lenaerts, J. T. M., Van De Berg, W. J. & Van Den Broeke, M. R. A 21st century warming threshold for sustained Greenland ice sheet mass loss. *Geophys. Res. Lett.* **48**, e2020GL090471 (2021).
40. Perrette, M., Landerer, F., Riva, R., Frieler, K. & Meinshausen, M. A scaling approach to project regional sea level rise and its uncertainties. *Earth Syst. Dynam.* **4**, 11–29 (2013).
41. Bilbao, R. A. F., Gregory, J. M. & Bouttes, N. Analysis of the regional pattern of sea level change due to ocean dynamics and density change for 1993–2099 in observations and CMIP5 AOGCMs. *Clim. Dynam.* **45**, 2647–2666 (2015).
42. Palmer, M. D. et al. *UKCP18 Marine Report* (Met Office, 2018); https://www.metoffice.gov.uk/pub/data/weather/uk/ukcp18/science-reports/UKCP18-Marine-report.pdf
43. Church, J. A. et al. in *Climate Change 2013: The Physical Science Basis* (eds Stocker, T. F. et al.) 1137–1216 (Cambridge Univ. Press, 2013).
44. Levermann, A. et al. Projecting Antarctic ice discharge using response functions from SeaRISE ice-sheet models. *Earth Syst. Dynam.* **5**, 271–293 (2014).
45. DeConto, R. M. & Pollard, D. Contribution of Antarctica to past and future sea-level rise. *Nature* **531**, 591–597 (2016).
46. DeConto, R. M. et al. The Paris Climate Agreement and future sea-level rise from Antarctica. *Nature* **593**, 83–89 (2021).
47. Meinshausen, M. et al. The RCP greenhouse gas concentrations and their extensions from 1765 to 2300. *Clim. Change* **109**, 213–241 (2011).
48. Nauels, A. et al. Multi-century global and regional sea-level rise commitments from cumulative greenhouse gas emissions in the coming decades [Dataset]. *Zenodo* https://doi.org/10.5281/zenodo.16572777 (2025).

Acknowledgements

J. Gregory is acknowledged for the development of the Monte Carlo code underlying the P20 sea-level model. We also acknowledge T. Edwards, R. Greve, A. Aschwanden and N. Golledge for leading research that resulted in reference datasets trialled and used for the MAGICC sea-level model update. T.H.J.H. and A.B.A.S. were supported by PROTECT. This project has received funding from the European Union Horizon 2020 research and innovation programme (grant no. 869304). This is PROTECT contribution no. 164. T.H.J.H. was also supported by the Netherlands Polar Programme of the Dutch Research Council. M.D.P. was supported by the Met Office Hadley Centre Climate Programme, funded by the Department of Science, Innovation and Technology (UK). T.M. acknowledges financial support by the Luxembourgish Fond National de la Recherche (under the AFR PhD grant no. 18824314). Z.N. acknowledges funding from the European Union Horizon 2020 research and innovation programme (grant agreement no. 101003536) (ESM2025).

Author contributions

A.N. designed the study, with input from M.D.P. and coordinated the research. A.N. and Z.N. led the scenario design. A.N., Z.N., T.M. and M.D.P. carried out the modelling. All authors (A.N., Z.N., T.M., T.H.J.H., M.M., U.K., C.S., A.B.A.S. and M.D.P.) contributed to the discussion and interpretation of the results. A.N. wrote the manuscript with input from Z.N., T.M., T.H.J.H., M.M., U.K., C.S., A.B.A.S. and M.D.P.

Competing interests

The authors declare no competing interests.

Additional information

Supplementary information The online version contains supplementary material available at https://doi.org/10.1038/s41558-025-02452-5.

Correspondence and requests for materials should be addressed to Alexander Nauels.

Peer review information *Nature Climate Change* thanks Michael Oppenheimer, Yona Silvy and the other, anonymous, reviewer(s) for their contribution to the peer review of this work.